

# Faraday Wave Pattern Selection Via Multi-Frequency Forcing

Jeff Porter\*

Department of Applied Mathematics, University of Leeds, Leeds LS2 9JT, United Kingdom

Chad M. Topaz

Department of Mathematics, U.C.L.A., Los Angeles, California 90095

Mary Silber

Department of Engineering Sciences and Applied Mathematics,  
Northwestern University, Evanston, Illinois 60208

(Dated: November 15, 2018)

We use symmetry considerations to investigate how damped modes affect pattern selection in multi-frequency forced Faraday waves. We classify and tabulate the most important damped modes and determine how the corresponding resonant triad interactions depend on the forcing parameters. The relative phase of the forcing terms may be used to enhance or suppress the nonlinear interactions. We compare our predictions with numerical results and discuss their implications for recent experiments. Our results suggest how to design multi-frequency forcing functions that favor chosen patterns in the lab.

PACS numbers: 05.45.-a, 47.35.+i, 47.54.+r, 89.75.Kd

Faraday observed in 1831 that patterns of subharmonic standing waves form on the surface of a fluid when its supporting container is shaken vertically with increasing strength [1]. The first Faraday wave experiments (see [2] for a review) used sinusoidal forcing to shake the fluid, and produced simple patterns (*e.g.*, stripes, squares, and hexagons). Remarkably, this experiment remains a rich source of intriguing new patterns, most recently as the basic sinusoidal forcing has been replaced by periodic functions with two or three frequency components. The two-frequency case has been investigated a great deal experimentally [3, 4, 5, 6, 7] and theoretically [8, 9, 10, 11], and has produced a variety of states, including superlattice patterns and localized structures, as well as the first experimental realizations of quasipatterns. Three-frequency forcing has been used too [3, 7], but to far less extent.

A primary focus of the past 10 years of investigation of one- and two-frequency forced Faraday waves has been on the role of resonant triad interactions – the lowest order nonlinear interactions – in pattern selection. A typical resonant triad consists of two critical modes and a third, damped mode with a distinct wavelength that determines the angle  $\theta_{\text{res}}$  between the critical wave vectors; see Fig. 1. It was originally thought that the damped mode should draw energy from the excited modes, creating an “anti-selection” mechanism that suppresses such triads in favor of patterns that avoid the resonant angle [12]. However, it has since been shown that the opposite effect may also occur. For instance, [10, 13] demonstrated for two-frequency forced Faraday waves that a damped mode oscillating at the difference of the two forcing frequencies is responsible for selecting the superlattice-I pattern reported in [6].

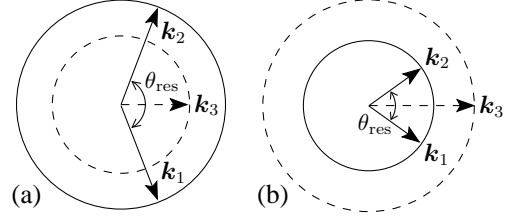


FIG. 1: Fourier space diagram of resonant triads composed of two critical modes ( $|\mathbf{k}_1| = |\mathbf{k}_2| = k_1$ ) and a damped mode ( $\mathbf{k}_3 = \mathbf{k}_1 + \mathbf{k}_2$ ,  $|\mathbf{k}_3| = k_3$ ) with (a)  $k_3 < k_1$ , (b)  $k_1 < k_3 < 2k_1$ . The resonant angle is given by  $\cos(\theta_{\text{res}}/2) = k_3/(2k_1)$ .

The richness of the Faraday system is due in large part to the vastness of the control parameter space which, in principle, is infinite-dimensional. By expanding an arbitrary periodic forcing function in a Fourier series

$$F(t) = f_m e^{im\omega t} + f_n e^{in\omega t} + f_p e^{ip\omega t} + \dots + c.c., \quad (1)$$

it is apparent that one has the freedom to choose the commensurate frequencies ( $m\omega, n\omega, p\omega, \dots$ ), the amplitudes ( $|f_m|, |f_n|, |f_p|, \dots$ ), and the phases ( $\phi_m, \phi_n, \phi_p, \dots$ ), where  $\phi_u = \arg(f_u)$ . Previous experimental and theoretical investigations have largely been exploratory in nature, *i.e.*, they have focused on describing the patterns which form at particular locations in parameter space. In this Letter, we take a prescriptive approach to pattern formation and demonstrate how the huge parameter space may be exploited to control resonant triads. In particular, we can either enhance or suppress triad interactions, largely at our discretion, by an appropriate choice of forcing frequencies, amplitudes, and phases.

Our analysis follows that of [11] which uses the (broken) symmetries of time translation, time reversal, and

Hamiltonian structure, and is valid near onset in weakly-damped systems. Our main result is a table summarizing, for up to three forcing frequencies, which damped modes are likely to be important, the manner in which their coupling with critical modes depends on the forcing parameters and, in many cases, the overall qualitative effect (enhancing or suppressing) they have on associated patterns. These results are then applied to two specific examples relevant to experiments. In the first, we show how the superlattice pattern selection mechanism discussed in [10, 13] may be dramatically enhanced by the addition of a third frequency component with appropriate phase. In the second, we offer an explanation for why a distorted 8-fold quasipattern observed with two-frequency forcing became much more regular and robust when a third forcing frequency component was applied in the experiments of [7].

We consider resonant triads composed of two critical modes and a third linearly damped mode (which may, nevertheless, be forced) oscillating with dominant frequency  $\Omega > 0$ . The particular values of  $\Omega$  most crucial to pattern selection will be determined in the course of our calculation. Time is rescaled so that the common frequency is one, and we take the  $m$  component of the forcing to drive the critical modes, which therefore have dominant frequency  $m/2$ . All other modes are linearly damped. We begin by expanding the fluid surface height  $h$  in terms of six traveling wave (TW) modes:

$$h(\mathbf{x}, t) = \sum_{j=1}^3 \sum_{\pm} Z_j^{\pm}(t) e^{i(\mathbf{k}_j \cdot \mathbf{x} \pm \varpi_j t)} + c.c. + \dots, \quad (2)$$

where  $\varpi_1 = \varpi_2 = m/2$  and  $\varpi_3 = \Omega$ . The TW amplitude equations respect the spatial symmetries of the problem (translation, reflection through  $\mathbf{k}_3$ , inversion through the origin) and the temporal symmetries

$$T_\tau : Z_j^{\pm} \rightarrow e^{\pm i \varpi_j \tau} Z_j^{\pm}, \quad f_u \rightarrow e^{i u \tau} f_u, \quad (3a)$$

$$\kappa : Z_j^{\pm} \leftrightarrow Z_j^{\mp}, \quad (t, \gamma) \rightarrow -(t, \gamma), \quad f_u \rightarrow \bar{f}_u. \quad (3b)$$

Here  $u$  denotes any of the frequencies  $\{m, n, p, \dots\}$  and  $\gamma = 2\nu k^2$  is a dimensionless damping parameter formed from the kinematic viscosity  $\nu$  and the characteristic wave number  $k(m/2)$ , determined by the hydrodynamic dispersion relation. Note that  $T_\tau$  and  $\kappa$  are not symmetries in the usual sense; time translation  $T_\tau$  is broken by the forcing and time reversal  $\kappa$  by the damping. Nonetheless, they are valid *parameter symmetries* of the problem.

The equivariant TW equations take the form

$$\dot{Z}_1^+ = v Z_1^+ - \lambda f_m Z_1^- + \mathcal{Q}_1(Z_2^{\pm}, Z_3^{\pm}) + \dots, \quad (4a)$$

$$\dot{Z}_3^+ = \varrho Z_1^+ - \mu F_{2\Omega} Z_3^- + \mathcal{Q}_3(Z_1^{\pm}, Z_2^{\pm}) + \dots, \quad (4b)$$

with the remaining four equations related by symmetry. The parametric forcing term  $F_{2\Omega}$  represents products of

the  $f_u$  whose frequencies sum to  $2\Omega$  ( $F_{2\Omega} = f_{2\Omega}$  when  $2\Omega$  forcing is present). The resonant terms

$$\begin{aligned} \mathcal{Q}_1 &= (Q_1 Z_3^+ + Q_2 Z_3^-) \bar{Z}_2^+ + (Q_3 Z_3^+ + Q_4 Z_3^-) \bar{Z}_2^-, \\ \mathcal{Q}_3 &= Q_5 Z_1^+ Z_2^+ + Q_6 (Z_1^+ Z_2^- + Z_1^- Z_2^+) + Q_7 Z_1^- Z_2^-, \end{aligned}$$

couple the two modes at quadratic order. The resonant coefficients  $Q_\ell$ , according to  $T_\tau$ , must transform as  $(Q_1, \bar{Q}_5) \sim e^{i(m-\Omega)\tau}$ ,  $(Q_2, Q_7) \sim e^{i(m+\Omega)\tau}$ ,  $(Q_3, \bar{Q}_4, \bar{Q}_6) \sim e^{-i\Omega\tau}$ . The dependence of the  $T_\tau$ -invariant coefficients  $v$ ,  $\lambda$ , etc., on  $\gamma$  and the  $f_u$ , is also determined by symmetry. In particular,  $\kappa$  forces most of them to be purely imaginary at leading order. However, if  $k_1$  and  $k_3$  are defined by the local minima of the neutral stability curves then the imaginary parts of  $v$  and  $\varrho$  (*i.e.*, the detunings) vanish at  $\gamma = 0$ . We will need only the leading term in each coefficient so we write

$$v = -v_r \gamma, \quad \varrho = -\varrho_r \gamma, \quad \lambda = i\lambda_i, \quad \mu = i\mu_i, \quad Q_\ell = i q_\ell F_\ell,$$

where  $v_r, \varrho_r > 0$  (they correspond to damping terms),  $\lambda_i, \mu_i > 0$  (see [14]),  $q_\ell \in \mathbb{R}$  and  $F_\ell$  denotes an appropriate product of the  $f_u$  (or unity). The critical value of  $|f_m|$  is  $\mathcal{O}(\gamma)$  and all  $|f_u|$  are assumed to be related by a finite  $\gamma$ -independent ratio, so that  $|f_u| \sim \gamma$ .

For a given damped mode, the task is to determine how the resonant coefficients  $Q_\ell$  depend on the  $f_u$ , then apply a standard reduction procedure at the bifurcation to standing waves (SW). The resulting two equations (truncated at cubic order) describe SW dynamics near onset:

$$\dot{A}_1 = \lambda A_1 + A_1 (a |A_1|^2 + (b_0 + b_{\text{res}}) |A_2|^2). \quad (5)$$

The equation for  $A_2$  is obtained by switching labels. The self-interaction coefficient  $a$  and the “nonresonant” part  $b_0$  of the cross-coupling coefficient are  $\mathcal{O}(\gamma)$ .

Of primary interest here is the contribution  $b_{\text{res}}$  makes to the cross-coupling coefficient in (5) as a result of the slaved modes  $Z_3^{\pm}$ . Loosely speaking, if  $b_{\text{res}} > 0$  the stability of patterns involving critical modes separated by the angle  $\theta_{\text{res}}$  will be enhanced, whereas  $b_{\text{res}} < 0$  has a suppressing effect [10]. Since we are interested only in damped modes that have a significant impact on (5), we consider those cases where  $b_{\text{res}}$  is  $\mathcal{O}(\gamma)$  or larger [17].

There are then two possibilities for obtaining large  $b_{\text{res}}$ . If some of the  $Q_\ell$  are  $\mathcal{O}(1)$  then  $b_{\text{res}}$  is  $\mathcal{O}(\gamma^{-1})$  and dominates in the limit  $\gamma \rightarrow 0$ ; this happens only for  $\Omega = m$  and is in essence a single-frequency phenomenon (the “first harmonic” resonance). If  $\Omega \neq m$  and some of the  $Q_\ell$  are  $\mathcal{O}(\gamma)$  then  $b_{\text{res}}$  is  $\mathcal{O}(\gamma)$ , and hence comparable to  $b_0$ . This occurs when  $\Omega \in \{2m, n, m \pm n, n - m\}$  for some frequency  $n$ . However, the  $\Omega = 2m$  mode may be ignored because for Faraday waves it has a wavenumber  $k_3 > 2k_1$  and so it cannot satisfy the necessary *spatial* resonance condition. Each of the remaining conditions on  $\Omega$  generates a particular type of coupling. For example, with  $\Omega = n - m$  we have  $F_2 = F_7 = f_n$ . If more than

one condition is satisfied, as when  $\Omega = n - m = m - p$ , there are more coupling terms (here one would also have  $F_1 = \bar{F}_5 = f_p$ ). The maximum number of conditions that  $\Omega$  can satisfy simultaneously is three.

In addition to the issue of coupling terms, it matters whether or not the damped mode is parametrically forced at  $\mathcal{O}(\gamma)$ . This forcing is present when there is a frequency  $2\Omega$  in  $F(t)$  and magnifies the resonance effect as it brings the damped mode closer to criticality. In addition, it leads to interesting phase dependence as the “usual” phase, dictated by  $f_{2\Omega}$ , competes with the phase of the nonlinear forcing  $Q_3$  (see Eqs. 4).

In Table I we give the leading contribution to  $b_{\text{res}}$  of the important damped modes for different choices of  $F(t)$  containing up to three frequencies  $(m, n, p)$ . To simplify the expressions therein, we define

$$\begin{aligned} \alpha_1 &= q_1 q_5, & \alpha_2 &= q_2 q_7, & \alpha_3 &= 2q_6(q_3 - q_4), \\ \alpha_4 &= q_1 q_7 - q_2 q_5, & \alpha_5 &= \epsilon_\lambda(2q_1 q_6 + q_5(q_3 - q_4)), \\ \alpha_6 &= \epsilon_\lambda(2q_2 q_6 - q_7(q_3 - q_4)), & \epsilon_\lambda &= \text{sign}(\lambda_i), \end{aligned} \quad (6)$$

and the functions

$$P_{2\Omega}(\Phi) = \frac{(|\varrho| + \mu_i |f_{2\Omega}| \sin \Phi)}{(|\varrho|^2 - |\mu_i f_{2\Omega}|^2)}, \quad (7)$$

$$R_{2\Omega}(\Phi_1, \Phi_2) = \frac{(|\varrho| \sin \Phi_1 + \mu_i |f_{2\Omega}| \cos \Phi_2)}{(|\varrho|^2 - |\mu_i f_{2\Omega}|^2)}. \quad (8)$$

There are four groupings in the table. The first shows the five important damped modes and their contribution to  $b_{\text{res}}$  when there is only one type of coupling at  $\mathcal{O}(\gamma)$  or lower and no parametric forcing  $f_{2\Omega}$ . In these cases there is no (leading order) dependence on the forcing phases. In the second section the same damped modes have been parametrically forced. The factor  $1/|\varrho|$  is then replaced by  $P_{2\Omega}(\Phi)$  of (7), a strictly positive oscillatory function ( $|\varrho| > |\mu_i f_{2\Omega}|$  for damped modes) with extrema at  $\Phi = \pm 90^\circ$ . Entries in the third section display two types of coupling, while the final two cases in the table have  $f_{2\Omega}$  forcing as well. Note that equivalent cases can be trivially generated from those in Table I by switching  $n$  and  $p$  and relabeling, for example  $(m, n, n - m)$ ,  $\Omega = p$  is equivalent to  $(m, n, m + n)$ ,  $\Omega = n$ .

Hamiltonian structure in the undamped problem has important consequences for the results in Table I. If one assumes that at  $\gamma = 0$  Eqs. (4) derive from a Hamiltonian  $\mathcal{H}$  through  $dZ_j^\pm/dt = \mp i\partial\mathcal{H}/\partial\bar{Z}_j^\pm$  (see, e.g., [15]) then  $q_1 = q_5$ ,  $q_2 = q_7$ , and  $q_3 = q_4 = q_6$ . When we allow for simple rescalings:  $(Z_1^\pm, Z_2^\pm) \rightarrow \eta(Z_1^\pm, Z_2^\pm)$ ,  $(Z_3^\pm) \rightarrow \xi(Z_3^\pm)$  with  $\eta, \xi \in \mathbb{R}$ , these conditions relax to  $q_1 = rq_5$ ,  $q_2 = rq_7$ , and  $q_3 = q_4 = rq_6$  (for some  $r > 0$ ), implying

$$\alpha_1 > 0, \quad \alpha_2 > 0, \quad \alpha_3 = 0, \quad \alpha_4 = 0. \quad (9)$$

Relations (9) mean that for simple couplings (the first two sections of Table I) the sign of  $b_{\text{res}}$  is determined, and thus one knows if the resonant triad has an enhancing or

suppressing effect on patterns involving  $\theta_{\text{res}}$ . The  $\Omega = m$  and  $\Omega = m \pm n$  modes are suppressing, the  $\Omega = n$  mode is inconsequential, and the  $\Omega = n - m$  mode is enhancing.

We now pursue the implications of Table I by examining two cases relevant to recent experiments. We compare our theoretical predictions with coefficients calculated numerically from the Zhang-Viñals Faraday wave equations [12], which describe weakly-damped fluids in deep containers. The calculation (see [10] for details) gives us the cross-coupling coefficient  $b = b_0 + b_{\text{res}}$  at the SW bifurcation and is independent of the symmetry arguments used here.

As our first example we consider the superlattice-I pattern observed with two-frequency  $(m, n) = (6, 7)$  forcing in the experiments of [6]. The wave vectors making up the pattern lie on the vertices of two hexagons, one rotated by an angle  $\theta_h < 30^\circ$  with respect to the other (see Fig. 3 in [10]). It was shown in [10] that the experimentally observed angle of  $\theta_h \simeq 22^\circ$  is related to a resonant triad at  $\theta \simeq 158^\circ$  ( $= 180^\circ - 22^\circ$ ) involving the  $\Omega = n - m$  mode. This is the most interesting of the damped modes because it gives  $b_{\text{res}} > 0$  and thus acts as a selection mechanism. Table I provides a means by which to enhance this effect, namely by parametrically forcing the damped mode via  $(m, n, 2n - 2m) = (6, 7, 2)$  forcing. In Fig. 2a we show  $b(\theta)$  for the phase  $\Phi = 90^\circ$  which optimizes the stabilizing effect at  $\theta_h \simeq 22^\circ$ . In Fig. 2b we show that parametrically forcing the difference frequency mode with this phase quadruples the stabilizing impact with respect to the two-frequency case used in the experiments. Note that if the wrong phase ( $\Phi = -90^\circ$ ) is chosen, the effect of the resonance will actually be diminished compared to the two-frequency case. Fig. 2c shows the sinusoidal dependence of  $b_{\text{res}}$  on  $\Phi$ , in excellent agreement with our predictions.

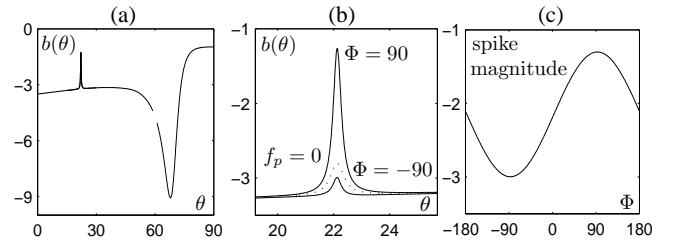


FIG. 2: Effect of  $\Phi$  on the stabilizing  $\Omega = n - m$  resonance that selects superlattice patterns [6] with  $(m, n, p) = (6, 7, 2)$  forcing. (a)  $b(\theta)$  with the optimal phase  $\Phi = 90^\circ$ ; the singular region heralding hexagons at  $\theta = 60^\circ$  is removed. The large dip near  $\theta = 67^\circ$  degrees is due to the strongly suppressing  $\Omega = m$  resonance in the first section of Table I. (b) Close-up of  $b(\theta)$  near  $\theta = 22^\circ$  with  $\Phi = 90^\circ$  and  $\Phi = -90^\circ$ ; the two-frequency result (dotted line) with  $f_p = 0$  is also shown. (c) Spike magnitude versus  $\Phi$  (see Eq. 7). For these calculations  $|f_n|/|f_m| = 0.75$ ,  $|f_p|/|f_m| = 0.1$ . The fluid parameters in the Zhang-Viñals equations of [12] are  $\gamma = 0.08$ ,  $G_0 = 1.5$ .

As a second example, we consider recent experimental

TABLE I: Leading resonant contribution  $b_{\text{res}}$  in (5) for the most important damped modes under appropriate choice of three-frequency forcing. Here,  $m, n, p, \Omega > 0$  and  $x \in \mathbb{Z}^+$ . Each expression for  $(m, n, p)$ , given  $\Omega$ , is excluded from those of entries further down the table. Dots in the first column indicate an arbitrary commensurate frequency. For  $\star$  the  $\pm$  follows sign  $(m - n)$ .

$(m, n, p)$	$\Omega$	Leading resonant contribution $b_{\text{res}}$	relevant phase(s)
$(m, \cdot, \cdot)$	$m$	$-\alpha_1/ \varrho $	
$(m, n, \cdot)$	$n$	$-\alpha_3 f_n ^2/ \varrho $	
$(m, n, \cdot)$	$m \pm n$	$-\alpha_1 f_n ^2/ \varrho $	
$(m, n, \cdot)$	$n - m$	$\alpha_2 f_n ^2/ \varrho $	
$(m, 2m, \cdot)$	$m$	$-\alpha_1 P_n(\Phi)$	$\Phi = \phi_n - 2\phi_m$
$(m, n, 2n)$	$n$	$-\alpha_3 f_n ^2 P_p(\Phi)$	$\Phi = 2\phi_n - \phi_p$
$(3x, 2x, \cdot)$	$x$	$-\alpha_1 f_n ^2 P_n(\Phi)$	$\Phi = 3\phi_n - 2\phi_m$
$(m, n, 2m \pm 2n)$	$m \pm n$	$-\alpha_1 f_n ^2 P_p(\Phi)$	$\Phi = \phi_p - 2\phi_m \mp 2\phi_n$
$(m, n, 2n - 2m)$	$n - m$	$\alpha_2 f_n ^2 P_p(\Phi)$	$\Phi = \phi_p + 2\phi_m - 2\phi_n$
$(m, n,  m - n )$	$n$	$(-\alpha_1 f_p ^2 - \alpha_3 f_n ^2 + \alpha_5 f_n  f_p \sin\Phi)/ \varrho $	$\Phi = \phi_n - \phi_m \pm \phi_p \star$
$(m, n, m + n)$	$n$	$(\alpha_2 f_p ^2 - \alpha_3 f_n ^2 + \alpha_6 f_n  f_p \sin\Phi)/ \varrho $	$\Phi = \phi_m + \phi_n - \phi_p$
$(m, n, 2m \pm n)$	$m \pm n$	$(\alpha_2 f_p ^2 - \alpha_1 f_n ^2 + \alpha_4 f_n  f_p \cos\Phi)/ \varrho $	$\Phi = 2\phi_m - \phi_p \pm \phi_n$
$(3, 1, 2)$	1	$-\alpha_1 f_p ^2 P_p(\Phi_1 - \Phi_2) - \alpha_3 f_n ^2 P_p(\Phi_1 + \Phi_2)$ $+ \alpha_5 f_n  f_p R_p(\Phi_1, \Phi_2)$	$\Phi_1 = \phi_n - \phi_m + \phi_p$ $\Phi_2 = \phi_m + \phi_n - 2\phi_p$
$(3, 2, 4)$	1	$-\alpha_1 f_n ^2 P_n(\Phi_1 + \Phi_2) + \alpha_2 f_p ^2 P_n(\Phi_2 - \Phi_1)$ $+ \alpha_4 f_n  f_p R_n(\Phi_1 - 90^\circ, \Phi_2 + 90^\circ)$	$\Phi_1 = \phi_n + \phi_p - 2\phi_m$ $\Phi_2 = 2\phi_n - \phi_p$

results on quasipatterns. It was reported in [7] that 8-fold quasipatterns, which were distorted and difficult to observe with  $(m, n) = (3, 2)$  forcing, became dramatically cleaner and more robust with  $(m, n, p) = (3, 2, 4)$  forcing. An explanation for this observation is provided by Table I. Specifically, we find that the  $\Omega = 1$  mode forms a resonant triad with the critical modes with associated angle  $\theta_{\text{res}} \approx 41^\circ$ . This is the angle present in the distorted (3,2)-forced quasipatterns in [7]. Table I indicates that with  $(m, n, p) = (3, 2, 4)$  forcing there is a positive  $\alpha_2|f_4|^2$  contribution to  $b_{\text{res}}$  which has a stabilizing effect. In our numerical investigations, we find that the stabilizing spike in  $b(\theta)$  becomes broader with increasing  $\gamma$ , and thus it is reasonable to expect that the stabilization could extend to the  $45^\circ$  angle associated with the perfect 8-fold quasipattern. Unfortunately, the experimental value of  $\gamma$  appears to be too large for a more quantitative comparison with our theory.

The theoretical framework developed in this Letter should provide some welcome guidance for navigating the huge parameter space of multi-frequency forced Faraday waves. Table I provides a comprehensive list of the important damped modes and their effect on pattern formation (additional possibilities with more than three frequencies will be considered elsewhere [16]). In general, the influence of these damped modes, when parametrically forced, depends on  $T_7$ -invariant combination(s) of forcing phases. Using the “proper” phase greatly enhances resonance effects while the “wrong” phase can actually reduce them. We hope that experimentalists will use Table I as a tool to design forcing functions conducive to particular patterns. For example, one might stabilize a quasipattern composed of  $2N$ ,  $N > 3$ , equally spaced critical modes by arranging for an  $\Omega = n - m$  mode with wavenumber  $k_3 = 2k_1 \cos(\frac{N-1}{N}90^\circ)$ . In the inviscid limit an appropriate choice of  $m$  and  $n$  can be estimated from this geometric condition and the dispersion relation [13]. Adding a third  $2n - 2m$  frequency would then allow one

to manipulate the effect by varying  $\Phi$ . Finally, we emphasize that the scheme used to obtain Table I is based on symmetry considerations and is therefore quite general, requiring only that the damping be small.

CMT was supported by NSF grants DMS-9983726 and DMS-9983320. MS was supported by NASA grant NAG3-2364, NSF grant DMS-9972059, and by the NSF MRSEC Program under DMR-0213745.

---

\* Electronic address: jport@maths.leeds.ac.uk

- [1] M. Faraday, Phil. Trans. R. Soc. Lond. **121**, 319 (1831).
- [2] J. Miles and D. Henderson, Ann. Rev. Fluid Mech. **22**, 143 (1990).
- [3] H. W. Müller, Phys. Rev. Lett. **71**, 3287 (1993).
- [4] W. S. Edwards and S. Fauve, J. Fluid Mech. **278**, 123 (1994).
- [5] H. Arbell and J. Fineberg, Phys. Rev. Lett. **81**, 4384 (1998).
- [6] A. Kudrolli, B. Pier, and J. P. Gollub, Physica D **123**, 99 (1998).
- [7] H. Arbell and J. Fineberg, Phys. Rev. E **65**, 036224 (2002).
- [8] T. Besson, W. S. Edwards, and L. Tuckerman, Phys. Rev. E **54**, 507 (1996).
- [9] W. Zhang and J. Viñals, J. Fluid Mech. **341**, 225 (1997).
- [10] M. Silber, C. M. Topaz, and A. C. Skeldon, Physica D **143**, 205 (2000).
- [11] J. Porter and M. Silber, Phys. Rev. Lett. **89**, 084501 (2002).
- [12] W. Zhang and J. Viñals, J. Fluid Mech. **336**, 301 (1997).
- [13] C. M. Topaz and M. Silber, Physica D **172**, 1 (2002).
- [14] J. Porter and M. Silber (2003), submitted to Physica D.
- [15] J. W. Miles, J. Fluid Mech. **146**, 285 (1984).
- [16] C. M. Topaz, J. Porter, and M. Silber (2003), in prep.
- [17] One can amplify the effect of modes with weaker coupling by bringing them extremely close to onset but this is effectively a *bicritical* situation which we avoid here.